A hand-held electrochemiluminescence biosensor for detection of carcinoembryonic antigen

Mohammadniaei, Mohsen; Zhang, Ming; Qin, Xianming; Wang, Wentao; Pia, Lorenza; Gürbüz, Hakan; Helalat, Seyed Hossein; Naseri, Maryam; Sun, Yi

Published in:
Talanta

Link to article, DOI:
10.1016/j.talanta.2023.125087

Publication date:
2024

Document Version
Publisher's PDF, also known as Version of record

Talanta 266 (2024) 125087

Contents lists available at ScienceDirect

Talanta

journal homepage: www.elsevier.com/locate/talanta

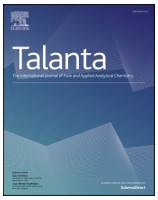

A hand-held electrochemiluminescence biosensor for detection of carcinoembryonic antigen

Mohsen Mohammadniaei [a,**], Ming Zhang [b], Xianming Qin [a], Wentao Wang [a], Lorenza Pia [a], Hakan Gürbüz [a], Seyed Hossein Helalat [a], Maryam Naseri [a], Yi Sun [a,*]

[a] Department of Health Technology, Denmark Technical University, Kgs. Lyngby, 2800, Denmark
[b] Jiangsu Engineering Research Center of Stomatological Translational Medicine, Nanjing Medical University, Nanjing, 210029, China

ARTICLE INFO

Keywords:
Electrochemiluminescence
Bipolar electrode
Carcinoembryonic antigen
ECL reporter
Parabolic reflector

ABSTRACT

After the development of portable glucose biosensor, challenges have remained to fabricate more portable devices for sensitive and reproducible detection of other biomarkers. Here, we fabricated a hand-held device for the quantification of carcinoembryonic antigen (CEA) or any other biomarkers based on electrochemiluminescence (ECL) using a bipolar electrode (BPE). The detection mechanism was based on a sandwich assay composed of a capture antibody and a secondary antibody conjugated with a robust ECL reporter. The ECL reporter was fabricated by conjugation of luminol on streptavidin-coated gold nanoparticle (Lum@SA-AuNP), leaving the biotin binding sites of the streptavidin intact for further conjugation with secondary antibody. This novel controlled functionalization strategy significantly enhanced the reproducibility and robustness of the biosensor. Moreover, an inventive parabolic reflector was implemented in the design, in order to maximize the lights to be captured by the photodiode (detector) and measured by a simple multimeter. Due to the synergetic signal amplification, the developed biosensor demonstrated a low sensitivity of 2.51 ng/ml with a linear detection range from 5 to 300 ng/ml with the ability to perform well in spiked-in samples. The designed sensing mechanism can definitely pave the way for further development of miniaturized devices in multiple formats.

1. Introduction

Cancer is still a leading cause of death worldwide. Tumor biomarkers, defined as biological or biochemical substances that are produced and secreted into body fluids, play an important role in cancer screening, disease progression detection, response to treatment, and monitoring of cancer recurrence. Carcinoembryonic antigen (CEA) is one of the most widely used tumor biomarkers. Overexpression of CEA is associated with several cancers including breast cancer, pancreatic cancer, lung cancer, and colon cancer [1]. Therefore, developing a sensitive, convenient, and accurate assay for CEA detection is crucial. Immunoassay has become the predominant analytical tool for the quantitative detection of CEA. However, traditional immunoassays are complex, time-consuming, expensive and require laboratory settings. To date, various immunoassay-based CEA biosensors have been developed for point-of-care use [2]. Optical and electrochemical biosensors are two widely used biosensing platforms, and several transducer types have been exploited, including surface-enhanced Raman scattering [3], chemiluminescence [4], fluorescence [5] and electrochemistry [6]. Despite of their promising features, both optical and electrochemical biosensors suffer from inherent limitations. For instance, fluorescence analysis requires an excitation light source, and is often affected by auto-fluorescence or a scattered light background; while electrochemical analysis is sensitive to working environment, thus lacks reproducibility and accuracy.

In that regard, electrochemiluminescence (ECL) that combines the advantages of both electrochemical and photoluminescence analysis is attracting more attention [7]. ECL is a process of electrogenerated chemiluminescence, and the detection is based on the light produced by an electron transfer reaction driven by a potential. It possesses unique characteristics, such as high controllability and fast measurement. Recently, a few ECL immunoassays have been developed for CEA detection. While most of these ECL biosensors consist of a three-electrode configuration, which is complex and imposes a negative

* Corresponding author.
** Corresponding author.
E-mail addresses: mniaei@gmail.com (M. Mohammadniaei), suyi@dtu.dk (Y. Sun).

https://doi.org/10.1016/j.talanta.2023.125087
Received 18 April 2023; Received in revised form 11 August 2023; Accepted 16 August 2023
Available online 16 August 2023

impact on practical applications [8]. One way to circumvent the issue is to explore the bipolar electrode (BPE)-based ECL. A BPE is simply a conductor, such as indium tin oxide (ITO) or Au, placed into a microfluidic channel [9]. In BPE-ECL, a driving potential is applied through an electrolyte solution containing a BPE, inducing faradaic reactions at the ends of the BPE. Compared to three-electrode ECL, BPE-ECL is much simpler and portable, thus have greater application potential in point-of-care testing. Another major challenge of ECL biosensors is that the luminol (co-reactant to produce ECL emission) is usually added in electrolyte solution, which limits the interactions between the target and ECL luminophore, hence impairing the detection sensitivity [10]. One promising solution to tackle this problem is to immobilize luminol molecules on nanoparticles, such as gold, silver and platinum nanoparticles [11]. These functionalized nanoparticles can accumulate on the electrode via the sandwich ELISA assay. Attributed to the catalytic properties and the high loading capability of nanoparticles, the sensitivity of ELC reaction could be greatly enhanced. However, it is very challenging to fabricate robust and reliable multifunctional nanoparticles with insignificant batch to batch variations.

In this study, we developed a hand-held device for the quantification of CEA biomarker using BPE-ECL (Fig. 1 left panel). The detection mechanism was based on a sandwich assay composed of a capture antibody and a secondary antibody conjugated with a robust ECL reporter. The novel ECL reporter was fabricated by conjugation of luminol on streptavidin-coated gold nanoparticle (Lum@SA-AuNP), leaving the biotin binding sites of the streptavidin intact for further conjugation with secondary antibody. This controlled functionalization strategy significantly enhanced the robustness and sensitivity of the biosensor. Moreover, an inventive parabolic reflector was implemented in the design, in order to maximize the light intensity to be collected by a simple photodiode (detector) and measured by a simple multimeter. Without using a relatively costly photomultiplier, the developed biosensor demonstrated an acceptable sensitivity of 2.51 ng/ml with a linear detection range from 5 to 300 ng/ml with the ability to perform well in spiked-in samples. Typically, a CEA level exceeding 2.9 ng/mL is deemed abnormal, but it does not essentially indicate the presence of cancer. The cutoff value for CEA is usually considered 5 ng/mL [12,13]. The innovative concept of using a parabolic reflector in a biosensing device together with the simple fabrication of a very robust ECL reporter can pave the way for further fabrication of miniaturized devices in multiple formats for commercial purposes.

2. Experimental

2.1. Reagents and apparatus

Carcinoembryonic antigen human (≥95% SDS-PAGE, buffered aqueous solution), alpha-fetoprotein, dibenzocyclooctyne-N-hydroxysuccinimidyl ester (DBCO-NHS ester), glutaraldehyde solution (GA, 25% in H_2O), phosphate buffer saline (10X PBS, pH 7.4), human serum albumin (HSA), bovine serum albumin (BSA), (3-aminopropyl) triethoxysilane (APTES), ethanol, luminol, hydrogen peroxide (H_2O_2), platinum sheet (20 mm × 20 mm × 1 mm), potassium ferricyanide, and Tween 20 were purchased from Sigma-Aldrich. Human CEA Antibody Pair (BSA and Azide free, ab270349) was purchased from Abcam Company. Streptavidin conjugated gold nanoparticles (SA-AuNP; 50 nm) were purchased from Nanocs, USA. ITO electrodes (10 mm × 2 mm × 1 mm; L × W × T) were purchased from National NanoFab Center (ROK), Korea. All chemicals were in analytical grade and used without further purification.

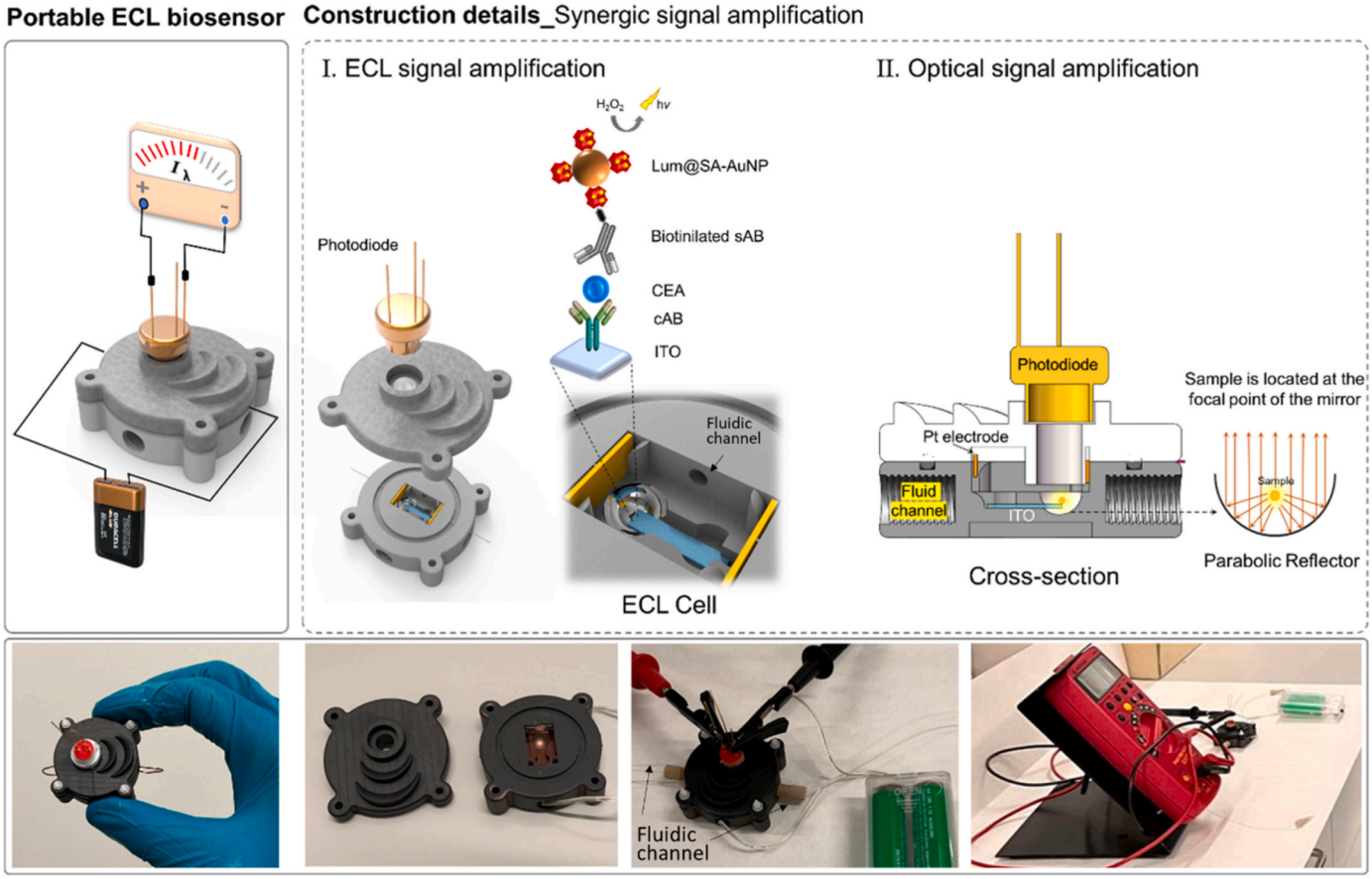

Fig. 1. Schematic diagram of the portable ECL biosensor, and the images of the prototype.

2.2. Fabrication of ECL reporter (Lum@SA-AuNP)

The ECL reporter was fabricated by conjugation of Luminol (Lum) to the amine group of streptavidins located at the surface of AuNPs, leaving the biotin sides of streptavidins intact. As illustrated in Fig. 2, an excess amount of DBCO-NHS ester (0.01 mg) was dissolved in 10 μL DMSO and slowly added in 50 μl of SA-AuNP (50 nM) followed by shaking for 2 h at room temperature (RT). This step turned all of the amine sides of streptavidin to cyclooctyne derivatives. The mixture was washed three times with 0.05% Tween-20 (in PBS) by centrifugation at 6000*g* for 6 min. Later, 0.05 mg Azide-NHS ester, which was thoroughly dissolved in 10 μL DMSO, was added to the mixture and incubated for 15 min at RT. This resulted in a click chemistry conjugation between the Azide group and the cyclooctyne derivatives, hence, formation of NHS groups on the streptavidins. The resulting mixture was washed three times by centrifugation at 6000*g* for 6 min and replacing the supernatants with 100 μL 0.05% Tween-20. Lastly, 0.05 mg Luminol was dissolved in 10 μL DMSO and added to the mixture. After 2 h incubation at 4 ^{O}C, the mixture was washed three times by centrifugation at 6000*g* for 6 min and replacing the supernatants with 100 μL 0.05% Tween-20 and stored at 4 ^{O}C for further use.

2.3. Construction of the portable ECL biosensor

A hand-held portable ECL biosensor was designed by Solidworks® software and printed using a 3D printer (Pico2 39, Asiga). As seen in Fig. 1 (right panel), the bipolar cell was designed to have a size of 14 mm × 7 mm × 7 mm (L × W × H). Two platinum electrodes (6.8 mm × 5 mm × 1 mm; L × W × T) were installed at both ends of the cell as the feeder electrodes and connected to a 4.5 V battery. The prepared ITO electrode was inserted inside the cell chamber, such that one end of the electrode (where the antibody is immobilized) was located at the focal point of the reflective mirror. The reflective mirror was made by coating 150 nm Au on the cell well (D = 6 mm) using a sputtering system with the base pressure of 7.5 × 10^{-7} Torr, in the presence of 20 SCCM (standard cubic centimetres/min) of Argon gas. Two fluidic channels were incorporated in the device for sample injection and cleaning purposes. The top and bottom part of the chamber were sealed-closed after the electrode insertion. A silicon photodiode (FDS010, Thorlabs Inc.; high speed, UV grade fused silica window with sensitivity down to 200 nm) was mounted at the top of the device and aligned to the end of the working electrode where the sample was located. The photodiode was connected to a digital multimeter to read the reverse signal.

2.4. Chemiluminescence setup

The chemiluminescence detection was performed using a real-time fluidic luminescence microplate reader (Agilent BioTek Synergy H1 Multimode Reader). A reaction mixture of 2 mM H_2O_2 and 5 mM potassium ferricyanide was prepared and inserted in the fluidic source. A sandwich assay was prepared on the ITO electrode composed of different volumes/concentrations of cAB, sAB, CEA and Lum@SA-AuNP. The prepared functionalized electrode was then inserted into a customized 3D printed plate (Supporting information Fig. S1). 100 μL PBS was added inside the wells and the plate was inserted into the reader. Next, using an optimized protocol, 100 μL of the reaction mixture (H_2O_2 and potassium ferricyanide) was dispensed into the wells at the rate of 300 μL/s, while the luminescence signal was recorded each 20 msec.

2.5. Functionalization of biosensor platform and sensing operation

The surface of ITO was functionalized with 10% APTES in ethanol for 2 h at RT. After rinsing thoroughly with MiliQ water, the electrode was treated with 5% glutaraldehyde for 1 h at RT. Next, the electrode was washed with MiliQ water three times and treated with 10 μl of capture antibody (cAB) against CEA at the concentration of 40 μg/ml and incubated overnight at 4 ^{O}C. After washing three times with washing buffer (PBS containing 0.05% Tween 20), the surface of electrode was treated with blocking buffer (1% BSA in PBS) for 1 h at RT. After three times rinsing with washing buffer, the electrode was incubated with 10 μL CEA for 2 h at RT. After the incubation, the electrode was washed with washing buffer and incubated with 10 μl of 20 μg/ml biotinylated secondary antibody (sAB) for 1 h at RT. It should be mentioned that the biotynilation of sAB was carried out using Biotinylation Kit (Fast, Type B) - Lightning-Link® (ab201796), according to the manufacturer protocol. Next, the electrode was washed with washing buffer and treated with 10 μl of Lum@SA-AuNP for 1 h at RT in a dark humid chamber. The electrode was then washed and inserted inside the ECL device. After closing and sealing the device, the cell was filled with 2 mM H_2O_2 in PBS (pH 8.5) using the fluidic channel. We had to seal the cell first then fill it with the buffer, otherwise the cell was not fully filled resulting in signal drifts. A constant DC voltage (E_{tot}) of 4.5 V was applied between the feeder electrodes and the ECL signal was read by a photodiode and recorded using a multimeter.

3. Results and discussions

3.1. Characterization of Lum@SA-AuNP

As illustrated in Fig. 2, the ECL reporter (Lum@SA-AuNP) was fabricated by conjugation of luminol on the streptavidin molecules that were coated on the surface of AuNP. Lum@SA-AuNP was fabricated using different concentrations of luminol (from 0.01 to 0.1 mg) and their luminescence signals were compared. As seen in Fig. 3a, dispensing the reaction mixture inside the wells resulted in a sharp increase in the CL signals within 2 s, following by a sudden drop in 3 s and gradual demolish after c.a. 10 sec. As shown in Fig. 3a and b, increasing the luminol concentration was followed by enhancement in the luminescence signal, before reaching at its maximum level at 0.05 mg. Therefore, 0.05 mg of luminol was used as the optimum concentration of luminol when used for conjugation with SA-AuNP.

To evaluate the number of the Streptavidin proteins on the surface of the AuNPs, we investigated the protein concentration in the utilized AuNP samples with BCA protein concentration assay kit. To this end, a

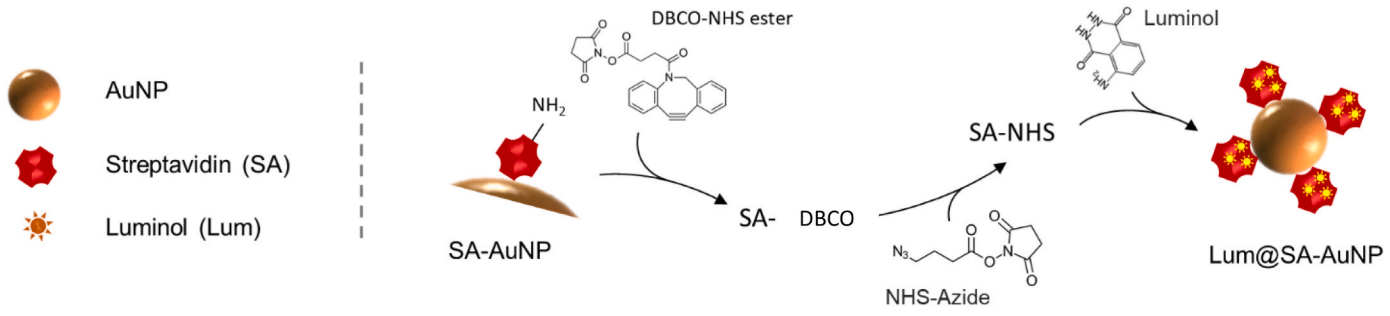

Fig. 2. Schematic illustration of conjugation of luminol on the SA-AuNP.

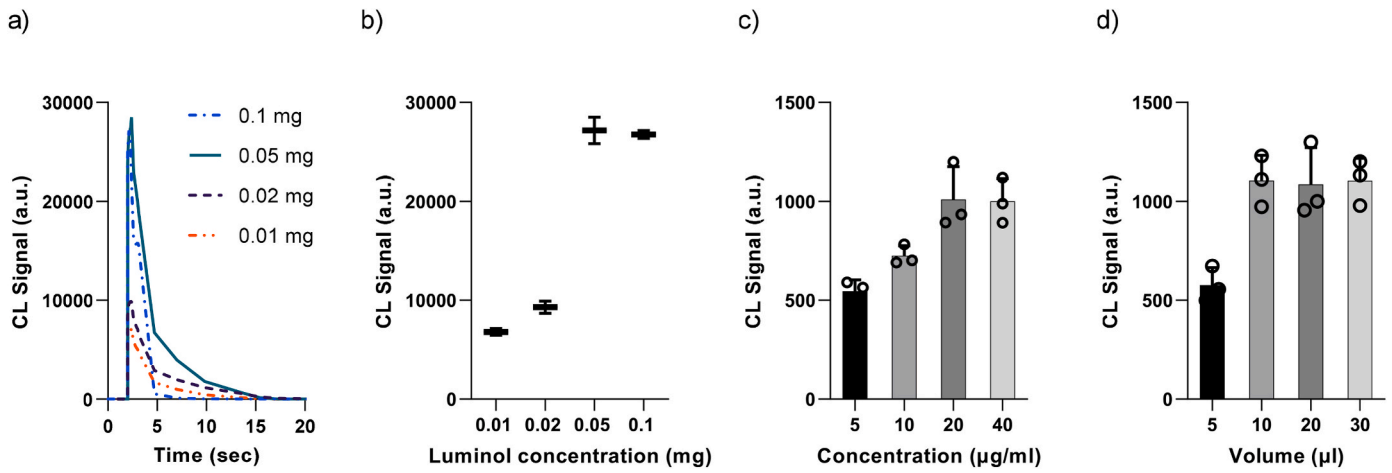

Fig. 3. (a) CL intensities recorded from 30 µL of Lum@SA-AuNP for various concentrations of luminol; (b) Bar chart describing a comparison between the maximum CL signals recorded from Lum@SA-AuNP for various concentrations of luminol; (c) Plotting the CL signal intensity arising from the reaction between the mixture of 2 mM H_2O_2/5 mM potassium ferricyanide with Luminol of the sandwich assay when detecting 5 ng/ml CEA at different concentrations of sAB and a fixed volume of Lum@SA-AuNP (20 µl); and (d) at different volumes of Lum@SA-AuNP and a fixed concentration of sAB (20 µg/ml). Error bars calculated from at least two replicates.

serial dilution of Streptavidin protein was prepared, and the related standard curve was created (Supporting information, Fig. S2). Afterwards, the nanoparticle sample's protein concentration was evaluated, and the average value of four separate tests was determined to be 185 µg/ml. By considering the molecular weight of Streptavidin (c.a. 52 kD), the total protein amount present was calculated (3560 nM). Furthermore, the manufacturer-provided data sheet indicated the concentration of the gold nanoparticles to be 50 nM. Based on the acquired results, around 70 Streptavidin proteins should be on the surface of each gold nanoparticle, which accounts for 280 luminol molecules on each gold nanoparticle. Although, this number should be lower due to the hindrance effect between luminol and free amine groups on Streptavidin.

Although it should be mentioned that there should be primary amine groups in the vicinity of biotin binding site, however, due to the fact that in our assay the Lum@SA-AuNP is added stepwise in the last step, there is a high chance that the biotinylated antibody conjugate with the target Lum@SA-AuNP. Moreover, the control functionalization mainly refers to the fact that we could have a robust functionalization of AuNP. Meaning that in contrast to the classical ratio-based stoichiometry assembly, here the number of luminol molecules on the AuNP are relatively fixed between the baches to provide less batch-to-batch variations.

3.2. Optimization of the biosensor components for CEA detection

The ECL device was used to optimize the concentration of secondary antibody (sAB) and Lum@SA-AuNP. An optimized amount of capture antibody (cAB) at the concentration of 40 µg/ml was immobilized on the end point of ITO electrode with the area of 4 mm^2. As seen in supporting information Fig. S3, at the fixed amounts of CEA (5 ng/ml), sAB (10 µg/ml), and Lum@SA-AuNP (20 µl), increasing the concentration of cAB from 10 to 60 µg/ml resulted in gradual increment in the CL signal where the maximum value was observed at 40 µg/ml. As evident, increasing the cAB concentration resulted in a slight decrease in the CL signal which can be due to the steric hindrance to hamper proper CEA capturing and thereby the sAB. Therefore, 40 µg/ml of cAB was chosen as the optimal value for further experiment.

To optimize the sAB concentration, the sandwich-based immunosensor was fabricated using different concentrations of sAB ranging from 5 µg/ml to 40 µg/ml, with CEA at a fix concentration of 5 ng/ml and Lum@SA-AuNP at a fixed volume of 20 µl. To reduce the variables and minimize extraneous factors for better optimization, we used CL measurement instead of ECL. Therefore, we used potassium ferricyanide to trigger the reaction instead of applying an external voltage. The reaction between potassium ferricyanide and hydrogen peroxide is often used as an oxidizing agent to trigger the chemiluminescence of luminol. When the two chemicals are mixed, they react to produce free radicals, which then react with luminol to produce a bright blue light. The overall reaction can be represented as follows:

$$K_3\,[Fe(CN)_6] + H_2O_2 + \text{luminol} \rightarrow \text{blue light}$$

As seen in Fig. 3c, the CL signal increased with the sAB concentration until 20 µg/ml where it was saturated. Therefore, 20 µg/ml of sAB was used as the optimum concentration for further analysis. Moreover, in order to optimize the Lum@SA-AuNP concentration, CEA and sAB were fixed at the concentrations of 5 ng/ml and 20 µg/ml, respectively. From the data shown in Figs. 3d and 10 µl of Lum@SA-AuNP gives the maximum CL value and was chosen as the optimum concentration for further experiments. Observing maximum CL value by adding 10 µl was due to the full surface coverage of the electrode effective area, not due to the saturation of sAB with Lum@SA-AuNP. We also performed the impact of Lum@SA-AuNP concentration on the CL signal by testing the serial dilutions of 10 µl Lum@SA-AuNP applied on the fixed concentrations of cAB (40 µg/ml), CEA (5 ng/ml) and sAB (20 µg/ml). As shown in supporting information Fig. S4, the stock concentration gave the highest CL value, while increasing the dilution factor was followed by gradual decrease in the CL signals. Therefore, 10 µl of the stock concentration of the Lum@SA-AuNP was used for further developments.

3.3. Design and optimization of the portable ECL biosensor

The design of the portable ECL biosensor was based on the bipolar electrochemistry (BE). As illustrated in Fig. 4a, applying a constant potential (E_{tot}) between the two feeder electrodes generates a linear potential gradient across the BPE. This creates an identical potential difference at both ends (anodic and cathodic) of the BPE (ΔE_{elec}), which leads to simultaneous faradaic reactions at both ends of the BPE without a direct ohmic contact. Therefore, application of a potential larger than the redox potential of an electroactive specie located at the anodic pole of the BPE, can lead to its oxidation. As shown, upon the application of potential, O_2 is reduced at the cathodic pole of the BPE, while Luminol is oxidized at the anodic pole to emit ECL.

In our design, we used an ITO electrode as a BPE, due to its conductivity and transparency. The constant potential was supplied by a

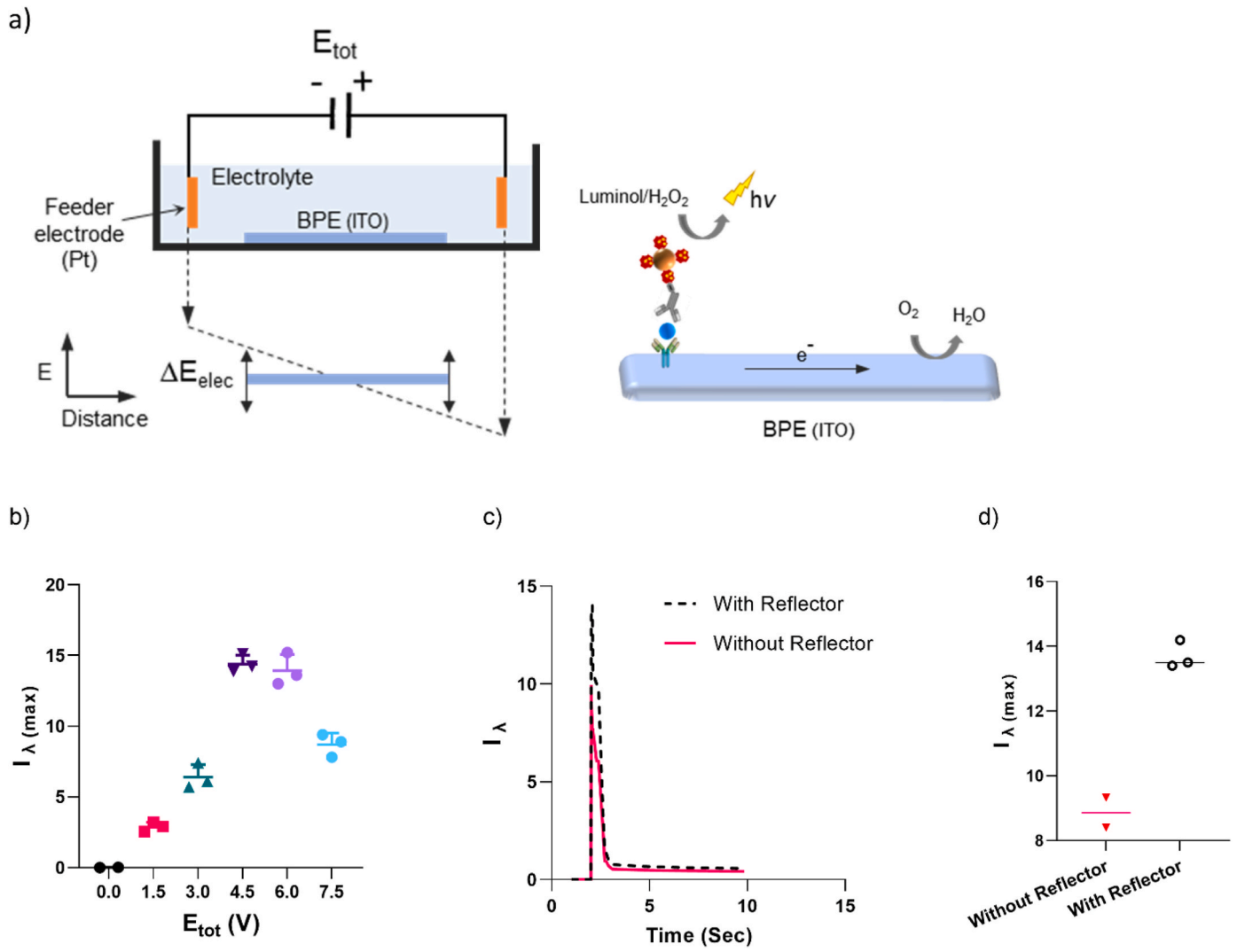

Fig. 4. (a) Schematic diagram of the BPE-ECL cell, illustrating the reaction mechanism inside the cell; (b) Maximum ECL signal intensity arising from luminol/H_2O_2 at different driving potentials (E_{tot}), for the detection of 300 ng/ml CEA using the portable biosensor; (c) Plotting the ECL intensity from 300 ng/ml CEA using the portable biosensor with/without the parabolic reflector; (d) Comparison between the maximum ECL intensities recorded for Fig. 4 B. Error bars were calculated from at least two replicates.

simple battery. We used a photodiode to read the ECL signals. Moreover, in order to enable the photodiode to capture all of the lights from the sample, we implemented a reflective surface under the ITO anodic pole. As seen in Fig. 1, the cell contains a round bottom reflective well. The well was designed so that the top surface of ITO electrode where the cAB is immobilized, was located at the focal point of the convex reflector, to mimic a parabolic reflector for ECL signal amplification.

To optimize the driving potential, the sandwich assay was formed at the anodic pole of the BPE and the ECL signal was recorded when applying different DC voltages (E_{tot}) from 0 to 12 V, which facilitated the reaction between the luminol on Lum@SA-AuNP and H_2O_2. The signal was measured by a photodiode connected to a multimeter. It should be mentioned that exposure of photodiode to light was followed by an increase in the reverse current (I_λ). In the absence of an incident light, I_λ is insignificant, contributing to a very low background signal hence high sensitivity. Fig. 4b illustrates the maximum ECL signals recorded from the portable biosensor when detecting 5 ng/ml CEA at different driving potentials. As shown, no signal was observed at the 0 V. However, increasing the E_{tot} was followed by gradual increase in the maximum ECL signal intensities where the highest signal was attributed to the 4.5 V sample. Increasing the voltage resulted in a drop in ECL intensity. This might be due to the fact that at high overpotential, oxidation of water and hydrogen peroxide (H_2O_2) are initiated to cause formation of bubbles. These bubbles can interfere with the ECL signal of luminol, which can affect the accuracy of the measurement. This is because the oxygen bubbles can trap the luminol and prevent it from reacting with the oxidant, reducing the amount of light emitted. Therefore, a 4.5 V battery was used for further experiments.

Moreover, to evaluate the role of reflector on the signal enhancement, two identical experiments were performed on two portable biosensors, one with the parabolic reflector and one without. From the results shown in Fig. 4c and d, an obvious signal enhancement of 24% was observed from the one with the reflector. The idea can pave the way for further development of more sensitive devices.

3.4. Analytical performance

The sensing performance of the developed device was based on the detection of ECL signal arising from luminol as a result of target detection. Higher concentration of CEA was followed by increment in the number of Lum@SA-AuNP on the surface of the electrode, hence higher ECL signals. As shown in Fig. 5a and b, increasing the CEA concentration led to increase in the ECL intensity. The fabricated ECL device showed a linear range from 5 ng/ml to 300 ng/ml (Fig. 5b). The limit of detection

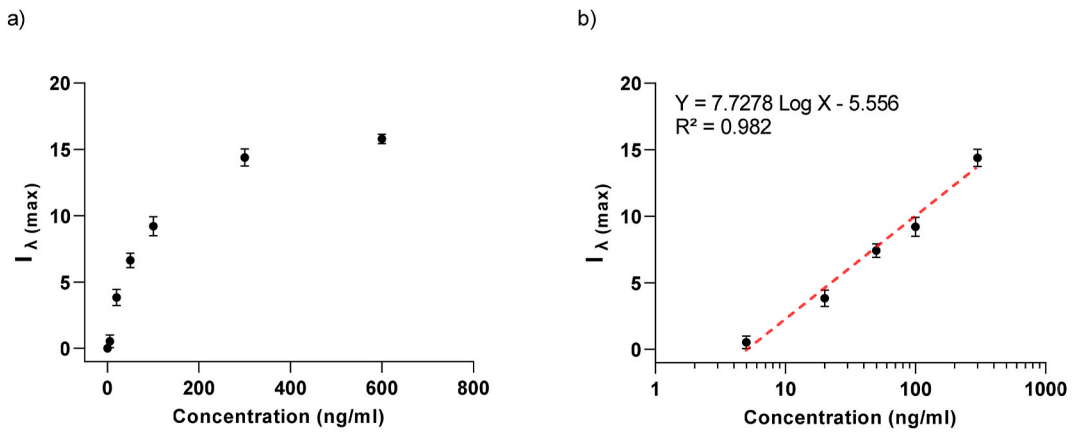

Fig. 5. (a) Typical ECL response of the portable device for the detection of serial concentrations of CEA at 0, 5, 20, 50, 100, 300, and 600 ng/ml in PBS buffer (pH 7.4); (b) Corresponding linear regression plot illustrating the maximum CEL signal intensity luminol as a function of CEA concentrations. Error bars were calculated from 3 replicates.

(LOD) and limit of quantitation (LOQ) were calculated 2.51 and 4.10 ng/mL, respectively. The concentration that produces a signal three or ten times higher than the standard deviations of the blank was defined as LOD or LOQ [14]. The low sensitivity of the biosensor can be due to the usage of a simple photodiode in our design or perhaps a simple ITO electrode without modification. Although compared to the other methods (Table 1), our device has a lower sensitivity, its superior robustness and simplicity is remarkable. We have remarkably reduced the batch-to-batch variations for constructing the signal reporter to reinforce the biosensor reproducibility. We did not use silver-based nanostructures which are prone to oxidization hence signal drifts. Moreover, we have introduced a portable device equipped with a parabolic reflector to be inspired by further researchers and to be implemented in the commercial devices to improve their sensitivity.

Specificity of the biosensor was also evaluated using different proteins of alpha-fetoprotein (AFP) and BSA. We wanted to make sure that BSA as the blocking agent does not interfere with the measurement. AFP and CEA are somewhat analogous in that they are both tumor markers that can be elevated in the blood of patients with certain types of cancer [12,23]. As shown in Fig. 6a, compared with CEA, the signals detected for BSA and AFP were very minimal, which clearly illustrated a high selectivity of the fabricated biosensor. For the stability test, four sets of electrodes immobilized with the cAB together with one batch of Lum@SA-AuNP were prepared. Electrodes and reagents were kept at 4 °C in a dark and humid chamber, to be used in their corresponding time points (0 day, 1 week, 2 weeks and 4 weeks). As seen in Fig. 6b, the ECL signals were significantly constant for 4 weeks, which can be attributed to the robustness of the electrodes and Lum@SA-AuNP. The relative standard deviation (RSD) for each measurement was less than 4.2% and the total RSD value over 4 weeks was 3.1% which demonstrated a high precision and reproducibility of the measurement. We also evaluated the batch-to-batch differences between each fabricated Lum@SA-AuNPs. As shown in Fig. 6c, very slight changes in the ECL signals for three batches was observed (RSD = 2.3%), demonstrating a very stable structure of Lum@SA-AuNP.

Furthermore, the capability of the developed biosensor to perform in human serum (HSA) was assessed. 20–100 ng/ml of CEA was spiked in 10% HSA (1:10 diluted in PBS) and the recovery rate was calculated. As shown in Table 2, the portable ECL device showed a sound recovery from 97.5% to 102.4%. The obtained data demonstrated the potential of our device to perform in real matrix. It should be noted that, we evaluated the spiked-in samples in 100% HAS, however, a poor recovery was

Table 1
Comparison study of different ECL based biosensors for CEA detection. Abbreviations: glassy carbon electrode (GCE), gold (Au), silver (Ag), Ruthenium (Ru), gold nanoparticle (AuNP), quantum dot (QD), nanoparticle (NP), carbon quantum dots (CQDs)poly (ethylenimine) functionalized graphene oxide (PEI-GO), screen printed electrode (SPE).

Electrode architect	Controlled functionalization	LOD (ng/mL)	Linear range (ng/mL)	Robustness	Simplicity	Device fabrication	Ref.
GCE/Au–Ag/g-C_3N_4	No	8.9×10^{-7}	$1–1 \times 10^{-6}$	Low, due to the usage of silver-based nanostructure	Very complex nanostructure synthesis procedure	No	[15]
Ru-graphene-Nafion/AuNP/QD	No	2×10^{-6}	5×10^{-4} - 5×10^{-6}	Low	Complex	No	[16]
Magnetic Fe_3O_4@Au NP/Ru@SiO_2	No	3.5×10^{-6}	$10–10^{-5}$	Low, due to multiple modification steps	Very complex, multiple enzymes	No	[17]
luminol functional-Au NPs@polypyrrole	No	3×10^{-6}	$10–10^{-4}$	Moderate	Moderate	No	[18]
porous partially reduced graphene oxide	No	2.6×10^{-6}	$10–10^{-5}$	Low, due to multiple modification steps	Complex	No	[19]
GCE-AgNPs/AuNPs/CQDs-PEI-GO	No	1.67×10^{-3}	$500–5 \times 10^{-3}$	Low, due to the usage of silver-based nanostructure	Complex	No	[20]
SPE-AuNPs-Ru-Arg@NH_2–Ti_3C_2-MXene/Ab/BSA/CEA	No	1.5×10^{-3}	$150–10^{-2}$	Low	Complex	No	[21]
GR-IL-Pt/Ti_3C_2 MXenes-Au NPs	No	3.5×10^{-5}	$10–10^{-4}$	Low	Complex	No	[22]
ITO/Lum@SA-AuNP	Yes	2.51	5–300	High	Simple	Yes	Present work

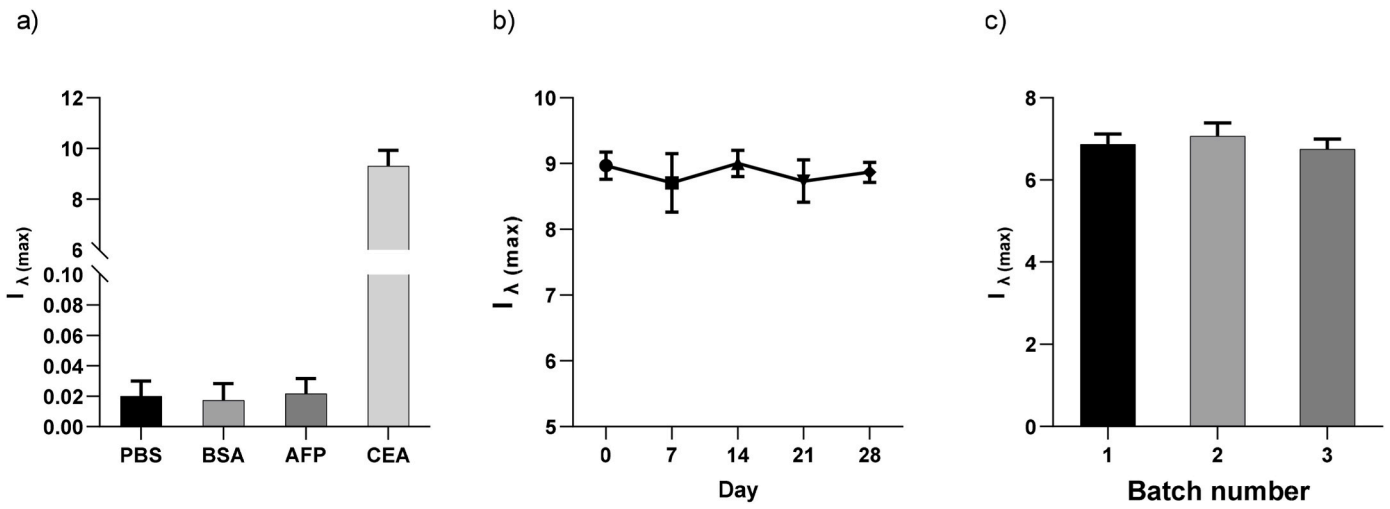

Fig. 6. (a) Specificity test of the CEA biosensor for the detection of BSA (5 μg/ml), AFP (5 μg/ml), and CEA (100 ng/ml); (b) ECl signals recorded from the portable device when detecting 100 ng/ml CEA at the first day of electrode preparation, after 7 days, 14 days, 21 days and 28 days storage at 4 °C; (c) ECL intensity recorder for the detection of 50 ng/ml CEA when the sandwich assay was directed to different batches of fabricated Lum@SA-AuNP. Error bars were calculated based on at least 2 replicates.

Table 2
Results from the calculation of CEA recovery rates in human serum at different spiked-in concentrations of 20, 50 and 100 ng/ml.

Sample number	Spiked-in CEA conc. (ng/ml)	ECL signal in 10% HSA	Calculated conc. (ng/ml)	Recovery rate (%)
1	20	3.12	19.5	97.5
2	50	7.17	51.2	102.4
3	100	9.46	99.8	99.8

observed. This might be due to the surface interaction of serum components with the ITO surface, leading to drift in sensor response and decreased reproducibility. The problem can be later mitigated using alternative surface passivation techniques.

4. Conclusion

A portable ECL biosensing device was fabricated based on a BPE system and a robust ECL reporter for the sensitive quantification of any biomarker with high degree of reproducibility. The handheld device was equipped with a simple multimeter and a 4.5 V battery, for the detection of CEA. A synergetic signal amplification strategy was implemented in the design based on Lum@SA-AuNP and a parabolic reflector. The Lum@SA-AuNP allowed controlled functionalization of luminol on the surface of AuNP to enhance the ECL signal arising from luminol upon the target recognition, while the parabolic reflector provided a secondary signal amplification by collecting most of the luminol luminescence lights. The fabricated biosensor was simple, cost-effective and very robust. To further enhance the sensitivity of the device, one can implement a photomultiplier in the design, or use different reflecting materials and perform more optimizations. Although, the assay still needs more optimizations to reduce the reaction times, by introducing new conjugation chemistries or better control on the sandwich formation using a multichannel fluidic system. The unique design of the portable ECL device can inspire more researchers to fabricate multiple and more sensitive universal platforms.

Credit author statement

Mohsen Mohammadniaei: Conceptualization, Methodology, Investigation, Writing – original draft. Ming Zhang: Investigation, Resources. Xianming Qin: Investigation, Resources. Wentao Wang: Investigation, Resources. Lorenza Pia: Investigation, Resources. Hakan Gürbüz: Investigation, Resources. Seyed Hossein Helalat: Investigation. Maryam Naseri: Investigation, Resources. Yi Sun: Writing- Reviewing and Editing, Supervision, Funding acquisition.

Declaration of competing interest

The authors declare that they have no known competing financial interests or personal relationships that could have appeared to influence the work reported in this paper.

Data availability

No data was used for the research described in the article.

Acknowledgment

This study was supported by the Innovation Fund Denmark, 8127-00021 B, and NovoNordisk Fonden, NNF21OC0070706.

Appendix A. Supplementary data

Supplementary data to this article can be found online at https://doi.org/10.1016/j.talanta.2023.125087.

References

[1] J. Nan, J. Li, X. Li, G. Guo, X. Wen, Y. Tian, Preoperative serum carcinoembryonic antigen as a marker for predicting the outcome of three cancers, Biomark. Cancer 9 (2017), https://doi.org/10.1177/1179299x17690142, 1179299X1769014.
[2] B.A.A. Manaf, S.P. Hong, M. Rizwan, F. Arshad, C. Gwenin, M.U. Ahmed, Recent advancement in sensitive detection of carcinoembryonic antigen using nanomaterials based immunosensors, Surface. Interfac. 36 (2023), 102596, https://doi.org/10.1016/j.surfin.2022.102596.
[3] C. Song, S. Guo, S. Jin, L. Chen, Y.M. Jung, Biomarkers determination based on surface-enhanced Raman scattering, Chemosensors 8 (2020) 1–15, https://doi.org/10.3390/chemosensors8040118.
[4] D.W. Jekarl, S. Lee, H. Park, H. Chae, M. Kim, Y. Kim, Analytical and clinical evaluation of chemiluminescent carcinoembryonic antigen (CEA) by HISCL-5000 Immunoanalyzer, Ann. Clin. Lab. Sci. 50 (2020) 417–422.
[5] L. Ding, X. Chen, L. He, F. Yu, S. Yu, J. Wang, Y. Tian, Y. Wang, Y. Wu, L.e. Liu, L. Qu, Fluorometric immunoassay for the simultaneous determination of the tumor markers carcinoembryonic antigen and cytokeratin 19 fragment using two kinds of CdSe/ZnS quantum dot nanobeads and magnetic beads, Microchim. Acta 187 (2020), https://doi.org/10.1007/s00604-019-3914-7.

[6] X. Gu, Z. She, T. Ma, S. Tian, H.B. Kraatz, Electrochemical detection of carcinoembryonic antigen, Biosens. Bioelectron. 102 (2018) 610–616, https://doi.org/10.1016/j.bios.2017.12.014.
[7] E.M. Gross, S.S. Maddipati, S.M. Snyder, A review of electrogenerated chemiluminescent biosensors for assays in biological matrices, Bioanalysis 8 (2016) 2071–2089, https://doi.org/10.4155/bio-2016-0178.
[8] L. Shang, B.J. Shi, W. Zhang, L.P. Jia, R.N. Ma, Q.W. Xue, H.S. Wang, Ratiometric electrochemiluminescence sensing of carcinoembryonic antigen based on luminol, Anal. Chem. 94 (2022) 12845–12851, https://doi.org/10.1021/acs.analchem.2c02803.
[9] F. Mavré, R.K. Anand, D.R. Laws, K.F. Chow, B.Y. Chang, J.A. Crooks, R.M. Crooks, Bipolar electrodes: a useful tool for concentration, separation, and detection of analytes in microelectrochemical systems, Anal. Chem. 82 (2010) 8766–8774, https://doi.org/10.1021/ac101262v.
[10] M. Mayer, S. Takegami, M. Neumeier, S. Rink, A. Jacobi von Wangelin, S. Schulte, M. Vollmer, A.G. Griesbeck, A. Duerkop, A.J. Baeumner, Electrochemiluminescence bioassays with a water-soluble luminol derivative can outperform fluorescence assays, Angew. Chem. Int. Ed. 57 (2018) 408–411, https://doi.org/10.1002/anie.201708630.
[11] M. Shourian, H. Ghourchian, M. Boutorabi, Ultra-sensitive immunosensor for detection of hepatitis B surface antigen using multi-functionalized gold nanoparticles, Anal. Chim. Acta 895 (2015) 1–11, https://doi.org/10.1016/j.aca.2015.07.013.
[12] L. Gan, S. Ren, M. Lang, G. Li, F. Fang, L. Chen, Y. Liu, R. Han, K. Zhu, T. Song, Predictive value of preoperative serum AFP, CEA, and CA19-9 levels in patients with single small hepatocellular carcinoma: retrospective study, J. Hepatocell. Carcinoma 9 (2022) 799–810, https://doi.org/10.2147/jhc.s376607.
[13] H. Zhang, C. Li, F. Hu, X. Zhang, Y. Shen, Y. Chen, F. Li, Auxiliary diagnostic value of tumor biomarkers in pleural fluid for lung cancer-associated malignant pleural effusion, Respir. Res. 21 (2020) 1–7, https://doi.org/10.1186/s12931-020-01557-z.
[14] R.M. McCormick, B.L. Karger, Guidelines for data acquisition and data quality evaluation in environmental chemistry, Anal. Chem. 52 (1980) 2242–2249, https://doi.org/10.1021/ac50064a004.
[15] X. Wei, X. Qiao, J. Fan, H. Dong, Y. Zhang, Y. Zhou, M. Xu, Electrochemiluminescence biosensor for carcinoembryonic antigen detection based on Au-Ag/g-C3N4 nanocomposites, Arab. J. Chem. 15 (2022), 104092, https://doi.org/10.1016/j.arabjc.2022.104092.
[16] T. Hao, Z. Guo, S. Du, L. Shi, Ultrasensitive detection of carcinoembryonic antigen based on electrochemiluminescence quenching of Ru(bpy) 32+ by quantum dots, Sensor. Actuator. B Chem. 171–172 (2012) 803–809, https://doi.org/10.1016/j.snb.2012.05.074.
[17] G. Jie, J. Ge, X. Gao, C. Li, Amplified electrochemiluminescence detection of CEA based on magnetic Fe 3 O 4 @Au nanoparticles-assembled Ru@SiO 2 nanocomposites combined with multiple cycling amplification strategy, Biosens. Bioelectron. 118 (2018) 115–121, https://doi.org/10.1016/j.bios.2018.07.046.
[18] W. Zhu, Q. Wang, H. Ma, X. Lv, D. Wu, X. Sun, B. Du, Q. Wei, Single-step cycle pulse operation of the label-free electrochemiluminescence immunosensor based on branched polypyrrole for carcinoembryonic antigen detection, Sci. Rep. 6 (2016) 1–9, https://doi.org/10.1038/srep24599.
[19] F.Y. Nie, L. Shang, W. Zhang, L.P. Jia, R.N. Ma, Q.W. Xue, H.S. Wang, Cathodic electrochemiluminescence of Ru(bpy)32+ based on porous partially reduced graphene oxide for detecting carcinoembryonic antigen, J. Electroanal. Chem. 928 (2023), 117055, https://doi.org/10.1016/j.jelechem.2022.117055.
[20] N.L. Li, L.P. Jia, R.N. Ma, W.L. Jia, Y.Y. Lu, S.S. Shi, H.S. Wang, A novel sandwiched electrochemiluminescence immunosensor for the detection of carcinoembryonic antigen based on carbon quantum dots and signal amplification, Biosens. Bioelectron. 89 (2017) 453–460, https://doi.org/10.1016/j.bios.2016.04.020.
[21] W. Luo, Z. Ye, P. Ma, Q. Wu, D. Song, Preparation of a disposable electrochemiluminescence sensor chip based on an MXene-loaded ruthenium luminescent agent and its application in the detection of carcinoembryonic antigens, Analyst 147 (2022) 1986–1994, https://doi.org/10.1039/d2an00450j.
[22] L. Shang, X. Wang, W. Zhang, L.P. Jia, R.N. Ma, W.L. Jia, H.S. Wang, A dual-potential electrochemiluminescence sensor for ratiometric detection of carcinoembryonic antigen based on single luminophor, Sensor. Actuator. B Chem. 325 (2020), 128776, https://doi.org/10.1016/j.snb.2020.128776.
[23] F. Feng, Y. Tian, G. Xu, Z. Liu, S. Liu, G. Zheng, M. Guo, X. Lian, D. Fan, H. Zhang, Diagnostic and prognostic value of CEA, CA19-9, AFP and CA125 for early gastric cancer, BMC Cancer 17 (2017) 1–6, https://doi.org/10.1186/s12885-017-3738-y.